Quaternary Research (2017), **88**, 430–445.

doi:10.1017/qua.2017.68

Pleistocene deep-sea ostracods from the Oki Ridge, Sea of Japan (IODP Site U1426) and condition of the intermediate water

Tatsuhiko Yamaguchi[a]*, Kentaro Kuroki[b], Katsura Yamada[b], Takuya Itaki[c], Kaoru Niino[d], Isao Motoyama[d]

[a]Center for Advanced Marine Core Research, Kochi University, Monobe B200, Nankoku, Kochi 783-8502, Japan
[b]Department of Geology, Faculty of Science, Shinshu University, 3-1-1 Asahi, Matsumoto 390-8621, Japan
[c]Institute for Marine Resources and Environment, Geological Survey of Japan, AIST, Higashi 1-1-1, Tsukuba, Ibaraki 305-8567, Japan
[d]Department of Earth and Environmental Sciences, Yamagata University, Yamagata 990-8560, Japan

(Received November 27, 2016; Accepted July 24, 2017)

Abstract

The Sea of Japan (also termed the East Sea) has a circulation system isolated from the Pacific Ocean and East China Sea. The East Asian winter monsoon drives the circulation system and cools the Tsushima Warm Current (TWC) to form the Japan Sea Intermediate–Proper Water (JSIPW). The intermediate water conveys oxygen to deep-sea floors, which is available for benthic animals. During the Pliocene (3.5–2.8 Ma), Temperate Intermediate Water (TIW) was formed under the weak winter monsoon, and extinct ostracod TIW taxa were found. Little is known about early Pleistocene intermediate water and the extinction mode of benthic ostracods. We studied radiolarians and ostracods from deep-sea sediments between 2.0 and 1.3 Ma (Marine Oxygen Isotope Stage [MIS] 77 to MIS 41) at Integrated Ocean Drilling Program Site U1426, Sea of Japan. The ostracod faunas contained TIW and JSIPW taxa. The radiolarian subtropical-water taxa and the JSIPW ostracods indicate a small influx of the TWC and the JSIPW. The TIW occasionally expanded to the middle bathyal zone. By analogy with the relationship between the modern JSIPW and winter monsoon, weak winter monsoon possibly caused gentle temperature gradients in the water column and the expansion of the TIW. The JSIPW taxa expanded their ranges into the deep sea during interglacial periods.

Keywords: East Asian winter monsoon; Intermediate water; Japan Sea Intermediate–Proper Water; Ostracoda; Pleistocene; Sea of Japan

INTRODUCTION

The Sea of Japan (also termed the East Sea) is a marginal sea of the northwestern Pacific Ocean and has a circulation system that is isolated from those of the Pacific Ocean and East China Sea. The Tsushima Warm Current (TWC), which is a branch of the subtropical western boundary current (Kuroshio Warm Current), flows into the Sea of Japan through the Tsushima Strait (120 m in depth). The water of the TWC cools off Khabarovsk, in the northern part of the Sea of Japan, and sinks to form the intermediate and bottom waters. The cooling of the water is intensified by the Asian winter monsoon (Gamo et al., 2001). The intermediate and bottom waters are referred to as the Japan Sea Intermediate–Proper Water (JSIPW) and are characterized by a high oxygen content (>5 mL O_2/L) and a homogeneous density with a temperature of 0–2°C and a salinity of less than 34.06 psu (e.g., Senjyu, 1999). The turnover periods of the intermediate and bottom waters are estimated to be ~100 yr (e.g., Kumamoto et al., 1998). The circulation changed quickly in response to the Plio-Pleistocene glacial–interglacial climate changes (e.g., Tada, 1994; Tada et al., 1999; Itaki et al., 2004; Watanabe et al., 2007).

Tada (1994) outlined the Neogene and Quaternary oceanography of the Sea of Japan. The structures of the deep water mass altered in response to the interglacial and glacial sea level changes after 2.5 Ma. During the interglacial periods, the TWC flowed, the JSIPW was formed, and below the TWC the water masses mixed. During the glacial periods, the low-stand sea level led to the TWC being blocked at the Tsushima Strait. Low-salinity water was input from rivers and formed a cap on the sea surface. The structure of the water mass was stratified (Tada, 1994). Anoxic conditions ceased in the deep water and caused dark-colored sediments with less or no bioturbation. The sediments are called the "dark layers" and used as marker layers to correlate with core sediments in the Sea of Japan (e.g., Ikehara, 2015; Tada, R., Irino, T., Expedition 346 Scientists, unpublished data).

*Corresponding author at: Center for Advanced Marine Core Research, Kochi University, Monobe B200, Nankoku, Kochi 783-8502, Japan. E-mail address: tyamaguchi@kochi-u.ac.jp (T. Yamaguchi).

Preliminary conclusions of Plio-Pleistocene oceanography indicate repeated periods of circulation with convection of oxygen during the interglacial periods and a stagnant water mass with a lack of oxygen during the glacial periods. Recent works have revealed variations in circulation changes and seafloor environments in response to the changes in climate (e.g., Watanabe et al., 2007; Usami et al., 2013; Ortakand et al., 2015). Watanabe et al. (2007) studied the texture and fabric of sediment and inferred changes between five oceanographic modes after 160 ka. Usami et al. (2013) examined benthic foraminifera from deep-sea cores studied by Watanabe et al. (2007). Watanabe et al. (2007) and Usami et al. (2013) indicated variations in circulation, surface productivity, and oxygen content on the seafloors and correlated the variations with changes in the intensity of the Asian winter monsoon.

Little is known about the details of circulation changes and seafloor environments before 160 ka. Itaki (2016) summarized geochemical and microfossil data from ocean drilling cores and outcrops on land in Japan and revised the outline of paleoceanography after 3.5 Ma. He suggested that the pattern of the circulation clearly changed at ~1.7 Ma, as Gallagher et al. (2015) pointed out. There are few data on benthic microfossils that indicate conditions in the deep-sea water mass through 1.7 Ma. Kato (1992) examined benthic foraminiferal faunas after ~4 Ma at Ocean Drilling Program (ODP) Site 798, Oki Ridge. According to the data compiled by Itaki (2016), samples with benthic foraminifera are sporadic before 1.7 Ma. Ostracods are used as tracers of water masses (e.g., Cronin et al., 2002). In the Sea of Japan, Ozawa (2003) investigated the bathymetric distribution of ostracod species from the modern sediments and correlated the ostracod assemblages with the water masses. Irizuki et al. (2007) studied Pliocene (2.7–3.5 Ma) deep-sea ostracods from the Kuwae Formation in Niigata, central Japan, and inferred developments in the Temperate Intermediate Water (TIW) during the interglacial periods and in the coastal water during the glacial periods. They consider that the TIW was above seafloors in the lower sublittoral and upper bathyal zones and warmer than the JSIPW.

No studies have ever dealt with ostracods from deep-sea drilling cores in the Sea of Japan, although many studies on ostracods have addressed the shallow-marine faunas from the Plio-Pleistocene strata on the land at the coast of the Sea of Japan (e.g., Cronin et al., 1994; Ozawa and Kamiya, 2001; Yamada et al., 2002, 2005). Ostracods are more sensitive to the oxygen content than benthic foraminifera (Moodley et al., 1997; Braeckman et al., 2013). They cannot survive in suboxic and anoxic conditions. Moffitt et al. (2015) discussed changes in the oxygen content in the Santa Barbara basin after the last glacial maximum (15–16 ka) in terms of the abundance of ostracods. According to this study, the absence of ostracods indicates a low oxygen content (<0.4 mL O_2/L). Analyzing ostracods allows us to discuss changes in oxygen content on the seafloor.

During the Integrated Ocean Drilling Program (IODP) Expedition 346, drilling was carried out on the seafloor at a depth of 903 m on the Oki Ridge—namely, at IODP Site U1426 (Tada et al., 2015). This site comprises successive sediments after 7 Ma. Our aims were to reveal the deep-sea ostracod faunas through 1.7 Ma at Site U1426 and to discuss changes in the seafloor environments, water mass, and benthic community on the Oki Ridge during interglacial and glacial periods.

LOCATION, LITHOLOGY, AND AGE MODEL OF U1426 CORES

At Site U1426 (37°2.00′N, 134°48.00′E), four cores (holes A–D) were drilled on the seafloor of the Oki Ridge at a depth of 903 m (Tada et al., 2015; Fig. 1). The seafloor is in contact with the JSIPW, which has a temperature of less than 2°C and an oxygen content of 4–5 mL O_2/L (e.g., Ikehara, 1991).

The core sediments consist of intermediate-frequency alternating layers (on a scale of 3–5 m) of brown and olive-gray clay; brownish, olive-green, and greenish-gray biosiliceous-rich nannofossil ooze; biosiliceous-rich clay; and diatomaceous ooze (Tada et al., 2015). Eight types of sediment layer were observed. In the study, we unified seven of these types (with the exception of a tephra layer) into three types of sediment: biogenic siliceous ooze, biogenic calcareous ooze, and terrigenous sediments (Fig. 2). In our measurements, most of the sediments had sand contents of less than 5%. Among the physical property parameters (Tada et al., 2015), the color reflectance parameters L* and b* fluctuated between 17.1 and 63.5 and between –9.8 and 7.2, respectively. The gamma-ray attenuation bulk density ranged from –0.329 to 1.697 g/cm^3. These physical property parameters exhibit cyclic fluctuations.

For the core depth scale, we use "m composite core depth below seafloor (CCSF)–D patched Ver1," which consists of revised splice intervals (Tada, R., Irino, T., Expedition 346 Scientists, unpublished data) and is shown at the website (http://geos45.ees.hokudai.ac.jp/~irino/exp346stratigraphy/). The geologic age of the core sediments was determined by magnetostratigraphy, a volcanic ash layer, and marker layers. Tada et al. (2015) indicated the chron boundaries of the magnetostratigraphy at Site U1426. Using the "dark layers" and volcanic ash layers, the sediment cores between the IODP Expedition 346 sites are being correlated (Tada, R., Irino, T., Expedition 346 Scientists, unpublished data). They calculated the ages of the "dark layers," using radiometric ages of volcanic ash layers, magnetostratigraphy, and microfossil biostratigraphy. In the interval of 123–225 m CCSF, 14 dark layers were recognized (Table 1). The Ebisutoge-Fukuda tephra layer is recognized at 187.156–187.196 m CCSF-D patched Ver1 in hole A. Chron C2n and the top of C2An.1n are correlated with the intervals of 195.31 to 218.308 m CCSF-D patched Ver1 and 283.557 m CCSF-D patched Ver1, respectively. The datum events of the layers and magnetostratigraphy allow us to give dating of the sediment samples. The age model allows us to calculate the sedimentation rates, which were 6.29–29.12 cm/ka (Fig. 3).

https://doi.org/10.1017/qua.2017.68 Published online by Cambridge University Press

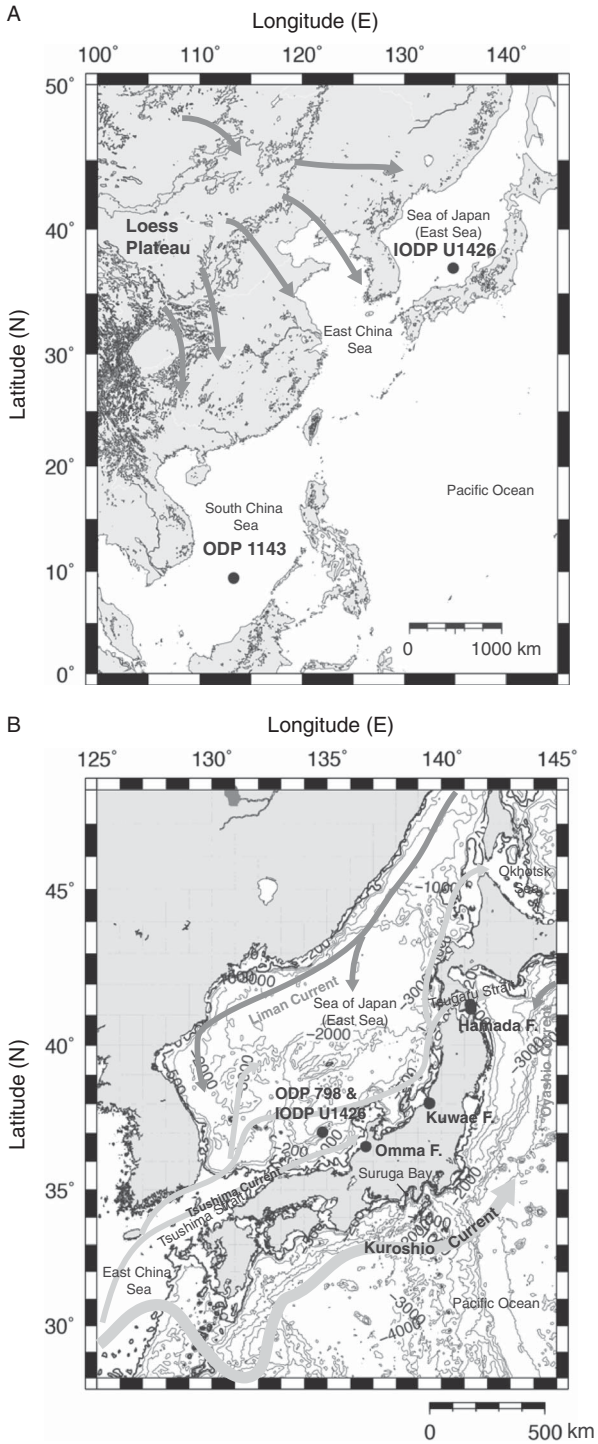

Figure 1. (A) Study and discussion sites and dominant wind vectors in winter during the East Asian winter monsoon. (B) Study and discussion areas and modern paths of ocean currents. F, formation; IODP, Integrated Ocean Drilling Program; ODP, Ocean Drilling Program.

MATERIALS AND METHODS

Sediment samples and extraction of ostracods

One hundred ninety-nine discrete samples with a volume of 34 cm^3 were taken at 50-cm intervals at a CCSF of 124.72–224.7 m in holes U1426A and U1426C. Applying the age model, the median of the time interval between the samples is estimated to be 3.0 ka. They were frozen under low pressure to dry before being washed with tap water through a 63 μm sieve. After the freeze-dried samples were washed, the samples from hole U1426A and hole U1426C were dried at room temperature and at less than 50°C, respectively, over two nights in an oven. Ostracods were obtained from the >150 μm fraction. To identify species, we used binocular microscopes and scanning electron microscopes at the Center for Advanced Marine Core Research, Kochi University and Shinshu University, Japan. We counted their abundance as the sum of the numbers of valves and carapaces. We obtained 414 carapaces and valve specimens from 87 of the 199 sediment samples and identified 26 taxa (Appendix A; Yamada et al., in press). Detailed data on the ostracods are shown in Yamada et al. (in press), including a list and scanning electron microscopy images of the ostracod taxa.

Ostracod taxa

The taxa include indicator species of two water masses: TIW taxa and JSIPW taxa. The TIW taxa, as proposed by Irizuki et al. (2007), consist of *Krithe antisawanensis* and *Krithe dolichodeira* [= *K. hemideclivata* of Zhao and Whatley (1997) and Irizuki et al. (2007); Ayress et al., 1999]. These taxa live in a water mass with a temperature of 6–20°C and a depth of 0–800 m in the East China Sea but do not inhabit the modern Sea of Japan. The TIW was warmer than the JSIPW and developed on seafloors in the lower sublittoral and upper bathyal zones (Irizuki et al., 2007). The JSIPW taxa, as defined by Ozawa (2003), comprise eight species: *Acanthocythereis dunelmensis*, *Argilloecia toyamaensis*, *Krithe reversa* [= *K. sawanensis* of Ozawa (2003); Coles et al., 1994], *Palmoconcha saboyamensis*, *Propontocypris uranipponica*, *Robertsonites hanaii*, and *R. tabukii* [= *R. reticuliforma* of Ozawa (2003); Irizuki et al. (2007)]. These taxa live in the JSIPW at a temperature of <5°C and a depth of 150–1500 m. Juveniles of *Krithe* species are regarded as *Krithe* spp. because it is difficult to identify them at the species level (Yamada et al., in press). Some specimens of *Krithe* spp. could belong to the TIW taxa. Using the sedimentation rates (cm/ka) and a sample volume of 34 cm^3, we calculated the benthic Ostracoda accumulation rates (BOARs) (ind./cm^2/ka), including those of the TIW taxa, the JSIPW taxa, and *Krithe* spp.

Statistics

To examine the relationship between the occurrence of ostracods, the oxygen content, and the export productivity, we subjected the L* values of the samples with and without ostracods and the BOAR values in the three types of sediment to statistical analyses. For a comparison of the brightness of the sediment color, the L* values of the two types of sample

https://doi.org/10.1017/qua.2017.68 Published online by Cambridge University Press

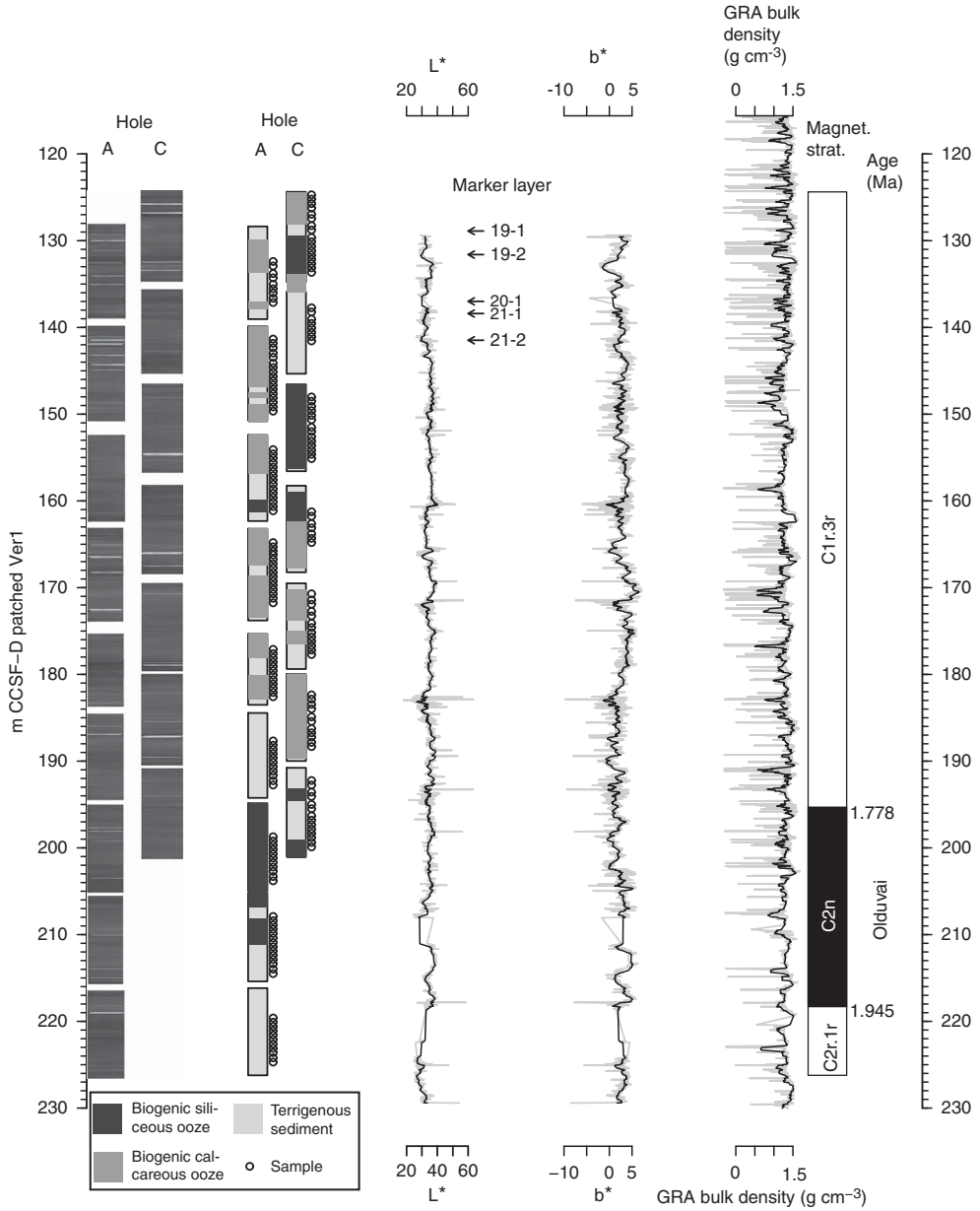

Figure 2. Images and types of lithology, stratigraphic position of samples, color reflectance parameters (L* and b*), gamma-ray attenuation (GRA) bulk density, and magnetostratigraphy. All the data are sourced from Tada et al. (2015). For the color reflectance and GRA bulk density data, the black curves represent 10-point moving averages. In the L*-depth plot, arrows indicate the dark layers (Tada, R., Irino, T., Expedition 346 Scientists, unpublished data). CCSF, composite core depth below seafloor.

were subjected to a permutation test. By performing a permutation test with 1000 iterations, the *P* value was calculated. To determine differences in the BOAR between the sediment types, the Steel-Dwass test with the Monte Carlo method was employed. A total of 56% of the discrete samples did not contain ostracods. The data for BOAR values were skewed and characterized by an abundance of zero values. For the assessment of data with abundant zero values, parametric methods such as the Student's *t*-test and Tukey's range test perform poorly because the mean is easily influenced by extreme values (Delucchi and Bostrom, 2004). Delucchi and Bostrom (2004) recommend nonparametric and resampling methods to avoid type I errors. We applied the Steel-Dwass test, which is a nonparametric method for multiple comparisons, to the BOAR values in the three types of sediment. Using the Monte Carlo method, the Steel-Dwass test was conducted 1000 times, and *P* values were calculated. The statistical analysis was performed using the free software R (R Core Team, 2015) and its package RcmdrPlugin.EZR (Kanda, 2013).

To illustrate the long-term changes in the BOAR values, the LOWESS (locally weighted scatterplot smoothing) filter was applied to the time series data of the values.

To identify periodicity in the ostracod abundance, we subjected the BOAR values and accumulation rates of the

https://doi.org/10.1017/qua.2017.68 Published online by Cambridge University Press

Table 1 . Datum events for the age model. CCSF, composite core depth below seafloor.

Event		Depth (m CCSF-D patched Ver1)	Age (Ma)	Reference	Remarks
Marker layer (cycle no.-dark layer no.)	17-1	119.71	1.192	Tada et al. (unpublished manuscript)	
	17-2	123.33	1.231	Tada et al. (unpublished manuscript)	
	18-1	125.385	1.256	Tada et al. (unpublished manuscript)	
	18-2	127.336	1.287	Tada et al. (unpublished manuscript)	
	19-1	128.886	1.311	Tada et al. (unpublished manuscript)	
	19-2	131.599	1.338	Tada et al. (unpublished manuscript)	
	20-1	136.994	1.406	Tada et al. (unpublished manuscript)	
	21-1	138.397	1.417	Tada et al. (unpublished manuscript)	
	21-2	141.477	1.455	Tada et al. (unpublished manuscript)	
Tephra	Ebisutoge-Fukuda	187.156	1.75	Irino et al. (unpublished manuscript)	U1426A-18H-6, 10–50 cm
Paleomagnetism	T C2n (Olduvai)	195.31	1.778	Tada et al. (2015)	U1426A-19H-5, 70 cm
	B C2n (Olduvai)	218.308	1.945	Tada et al. (2015)	U1426A-21H-7, 45 cm
	T C2An.1n (Matuyama/Gauss)	283.557	2.581	Tada et al. (2015)	U1426A-28H-6, 10 cm

TIW and JSIPW taxa to the multitaper method (MTM) of spectrum analysis (Thomson, 1982; Mann and Lee, 1996). Meyers (2012) developed the MTM of Mann and Lee (1996) to minimize its "edge effect" problem and simulated the method's suitability for time series data with noise. The modified MTM isolated and identified significant frequencies using the autoregressive-1 (AR1) "red noise" confidence interval and the MTM harmonic *F*-test confidence interval. According to Meyers (2012), we considered periodicities with probabilities of greater than 90% in the robust AR1 model and the MTM harmonic *F*-test. The analysis used a time–bandwidth product of 2, and the data were linearly detrended prior to analysis. Using the piecewise linear interpolation method, we interpolated the time series data of the BOAR, TIW, and JSIPW values at an even interval of 3.0 ka. The time series data were padded to 1260 points. The MTM of Mann and Lee (1996) was performed using the R package "astrochron" (Meyers, 2014).

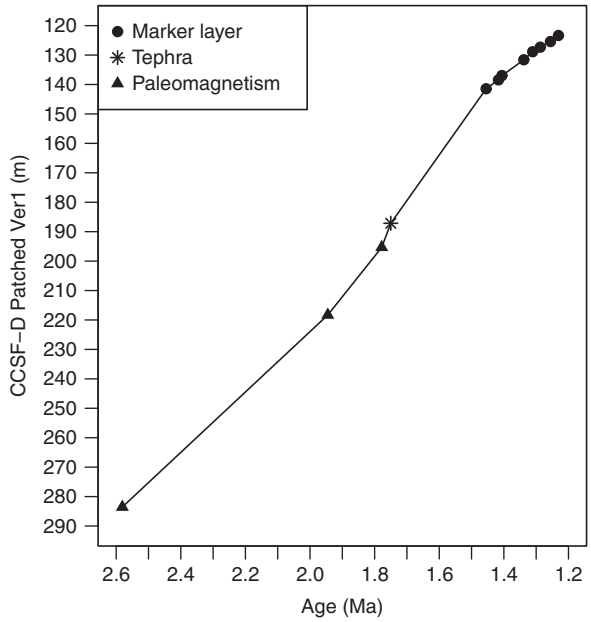

Figure 3. Age–depth model. Each circle corresponds to the depth and age of a discrete sample. The numerical values indicate the sedimentation rates. CCSF, composite core depth below seafloor.

Radiolarian subtropical water taxa

To recognize the inflow of the TWC, we examined the relative abundance of radiolarian taxa that are diagnostic for the TWC. These diagnostic taxa consist of the *Tetrapyle octacantha* group, the *Dictyocoryne* group, *Didymocyrtis tetrathalamus*, the *Euchitonia* group, and *Spongaster tetras* and are referred to as the subtropical water taxa. Today, these five taxa are distributed along the Kuroshio Warm Current in the tropical–subtropical Pacific (e.g., Lombari and Boden, 1985) and the East China Sea (Chang et al., 2003). In the southwestern part of the Sea of Japan, the relative abundances of the five taxa have higher values than anywhere else. They are correlated with the TWC (Motoyama et al., 2016). The relative abundance of the subtropical water taxa has been used to assess the flow of the TWC in the Sea of Japan during the late Pleistocene and Holocene (Itaki, 2007; Itaki et al., 2007; Itaki, T., Sagawa, T., Kubota Y., unpublished data). We made microscope slides from 95 sediment samples from hole 1426A, identified the five taxa among radiolarian assemblages with more than 200 specimens, and counted the five taxa and all the radiolarians (>45 μm).

Foraminifer and geochemical data for the Oki Ridge

To discuss the paleoenvironments on the Oki Ridge, we compared the ostracod data with the geochemical and benthic foraminifer data at ODP Site 798, Oki Ridge of Kheradyar

https://doi.org/10.1017/qua.2017.68 Published online by Cambridge University Press

(1992), Kato (1992), and Piper and Isaacs (1995, 1996). Site 798 is located at 37°2.310′N, 134°47.976′E and at a depth of 900 m. The site is located 0.6 km northwest of Site U1426. Piper and Isaacs (1995, 1996) measured trace elements such as molybdenum (Mo), uranium (U), vanadium (V), and chromium (Cr) in sediments from Site 798 and inferred that redox conditions were present on seafloors and in water columns between 1.40 and 1.28 Ma. These elements are sensitive to redox conditions and are correlated with the amounts of organic matter and the formation of pyrite (e.g., Tribovillard et al., 2006). Using their measurements, we calculated the V/Cr ratio, which is a proxy for redox conditions (Jones and Manning, 1994; Rimmer, 2004; Tribovillard et al., 2006). In our study, we used the classification of Tyson and Pearson (1991) of environments with different oxygen concentrations: 2–8 mL O_2/L for oxic, 0.2–2 mL O_2/L for dysoxic, and 0–0.2 mL O_2/L for suboxic conditions. Jones and Manning (1994) proposed values of the V/Cr ratio (ppm/ppm) for redox conditions: <2.0 for oxic, 2.0–4.25 for dysoxic, and >4.25 for suboxic conditions. The ratio may also indicate relative differences in redox conditions (Rimmer, 2004). The age model is based on magnetostratigraphy (Ingle et al., 1990; Hamano et al., 1992). Using the age model, the sedimentation rates were calculated to be between 12.82 and 13.15 cm/ka. Kheradyar (1992) and Kato (1992) studied planktic and benthic foraminifer assemblages, respectively. We plotted the relative abundance of *Globorotalia inflata* and *Globigerina ruber* in planktic foraminifer assemblages with more than 100 specimens in Kheradyar (1992). These species flourish in the channel of the Tsushima Strait (Domitsu and Oda, 2005). *G. inflata* and *G. ruber* indicate a warm intermediate water mass and the TWC influx, respectively (Kitamura and Kimoto, 2006; Kitamura, 2009). Using the relative abundance of this species, Kitamura (2009) has already discussed changes in the temperature of the intermediate water at the Oki Ridge. Using data from Kato (1992), we calculated the benthic foraminifer accumulation rate (BFAR), which is an indicator of export productivity (Herguera and Berger, 1991). Kato (1992) collected benthic foraminifera with a size of greater than 125 μm and measured the number of benthic foraminifer individuals per 1 g sediment (i.e., the foraminifer density). By multiplying by the foraminifer density, the dry bulk density in each section (Ingle et al., 1990), and the sedimentation rates, the BFAR values were calculated (Appendix C in the Supplementary Materials).

RESULTS

Ostracod taxa

Ostracods were present in series of 2–9 successive sediment samples and absent in series of 2–13 successive samples (Appendix B in the Supplementary Materials). In 56% of the samples, the abundance and BOAR value were zero. The remaining samples, which contained ostracods, had an abundance of 1–50 and a BOAR of 0.19–22.41. At a 186.306 m CCSF-D patched Ver1 (346-1426A-18H-5W, 75–77 cm), the abundance and BOAR reached maxima. Regarding the pattern of ostracod occurrence, ostracods were found in 30 series with 1–8 samples (1–35.5 ka in duration) but were not found in 31 series with 1–16 samples (1.5–104.5 ka in duration). *A. dunelmensis*, *R. tabukii*, and *Krithe* species were found frequently and were present in 78 samples. The JSIPW taxa occurred successively (Fig. 4) and were found in 29 series of the samples. Their presence continued for 3–355 ka. The TIW taxa appeared discontinuously in 16 samples, and their presence persisted for 1–8 ka (Table 2). The JSIPW taxa were not often associated with the TIW taxa. *Krithe* spp. were present in 30 discrete samples and 23 series with 1–3 samples (1–15 ka in duration).

Statistics

In a comparison of L* values between samples with and without ostracods, the permutation test rejected the null hypothesis that the L* values were equivalent for both types of sample. The median L* values were 35.25 for samples with ostracods and 34.0 for samples without ostracods (Fig. 5A). The *P* value from the permutation test was calculated to be 8.9×10^{-6}. The ostracod-bearing samples displayed significantly higher L* values than the other samples. In a comparison of the BOAR between biogenic siliceous ooze, biogenic calcareous ooze, and terrigenous sediment, we recognized significant differences in the BOAR between biogenic siliceous ooze and terrigenous sediment and between biogenic calcareous ooze and terrigenous sediment at a significance level of $P < 0.05$ (Table 2). The biogenic sediments contained significantly more ostracods than the terrigenous sediments. The median BOAR values were zero for biogenic siliceous ooze, 0.45 for biogenic calcareous ooze, and zero for terrigenous sediment (Fig. 5B). The 75th percentiles were 1.26 for biogenic siliceous ooze, 1.34 for biogenic calcareous ooze, and 0.45 for terrigenous sediment.

The LOWESS filter indicated declines in the BOAR from 1.90 to 1.86 Ma and from 1.70 to 1.67 Ma. The combination of the robust AR1 model and the MTM harmonic *F*-test identified a significant peak at confidence levels of 90% in the power spectra TIW values, which occurred at 15.18 ka (Fig. 6; Table 4). However, any peaks for the accumulation rates of the BOAR and JSIPW taxa were not significant.

Foraminifer, radiolarian, and geochemical data for the Oki Ridge

In the U1426 sediments, we observed calcareous benthic foraminifera in all the samples used for the analysis of ostracods. From the results for the radiolarians, the subtropical water taxa were found in 58 samples. The relative abundances of subtropical water taxa were less than 9.7%. At 1.2–1.4 Ma, the subtropical water taxa were not found. At 1.485–1.520, 1.619–1.660, and 1.712–1.775 Ma, the relative abundances often exceeded 1.0%. At 1.686 Ma, the relative abundance reached a maximum of 9.7%. Between 1.8 and

https://doi.org/10.1017/qua.2017.68 Published online by Cambridge University Press

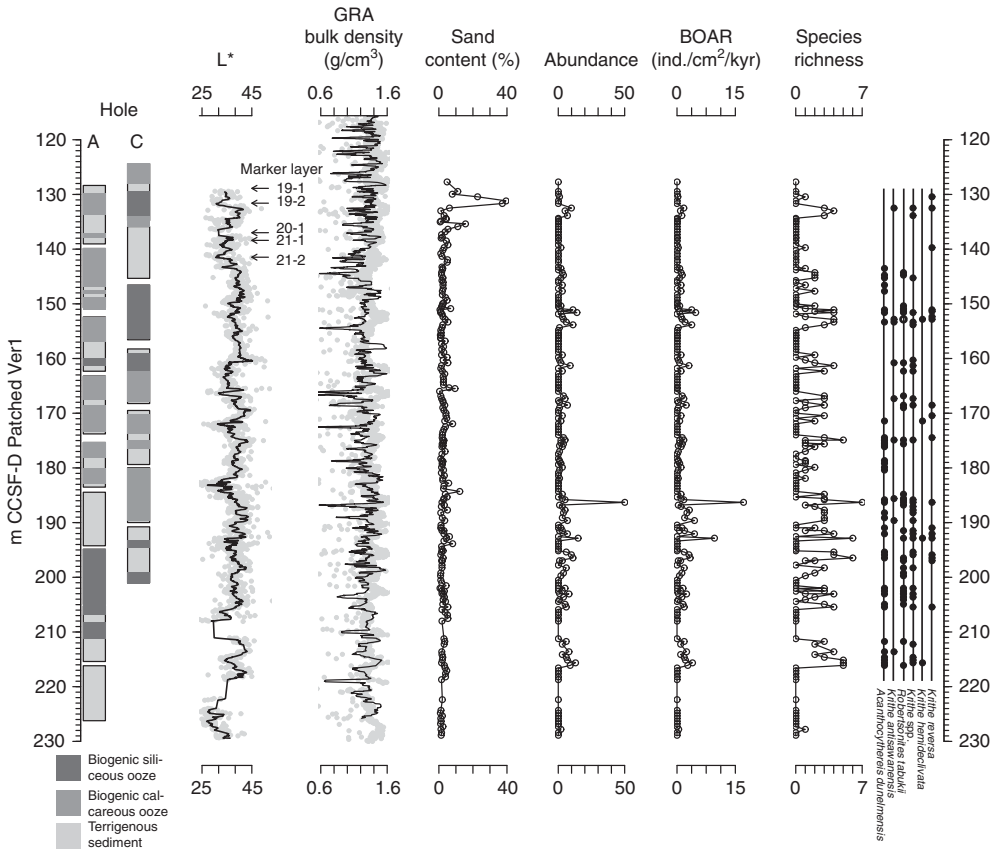

Figure 4. Lithology, color reflectance parameter L*, gamma-ray attenuation (GRA) bulk density, sand content, ostracod abundance, benthic Ostracoda accumulation rate (BOAR), species richness, and occurrence of six dominant taxa. The lithology, L*, and GRA data were sourced from Tada et al. (2015). For the color reflectance and GRA bulk density data, the black curves represent 10-point moving averages. In the L*-depth plot, arrows indicate the dark layers (Tada, R., Irino, T., Expedition 346 Scientists, unpublished data).

2.0 Ma, the subtropical water taxa often appeared and accounted for 0.3–1.0% of radiolarian assemblages.

From the geochemical data for ODP Site 798, Mo, U, and V displayed high values at 1.34–1.35 and 1.39–1.40 Ma. The peak values for Mo exceeded 40 ppm. The maximum values for U and V exceeded 5 ppm and 20 ppm, respectively (Piper and Isaacs, 1996; Fig. 7). The V/Cr ratio (ppm/ppm) ranged between 0.38 and 5.56 and exhibited plateaus with values of greater than 2.0 at 1.349–1.356 and 1.389–1.396 Ma. Peaks with values of greater than 4.25 were observed at 1.393 and 1.395 Ma. In the intervals between the plateaus, Mo, U, and V also exhibited high values. The BFAR fluctuated between 2 and 8852 (Fig. 8). The maximum BFAR appeared at 1.37 Ma. *G. inflata* appeared at ~1.55 Ma, exhibited two peaks in its relative abundance at 1.44 and 1.35 Ma, and disappeared at ~1.31 Ma (Fig. 8).

DISCUSSION

Ostracod responses to oxygen content and export productivity

All the sediments contained calcareous benthic foraminifera, although 56% of them lacked ostracods. The absence of ostracods was not caused by the dissolution of carbonate during diageneses.

Ostracods occurred in brightly colored sediments with higher L* values (Fig. 5A). Because the brightness of sediments is related to their biological productivity and oxygen content (Watanabe et al., 2007; Usami et al., 2013), the ostracod occurrence was linked to these environmental parameters. In the Sea of Japan, brightly colored sediments indicate oxic conditions and a high biogenic content (e.g., Tada et al., 1999; Watanabe et al., 2007). The occurrence of ostracods was correlated with high biogenic productivity and oxic conditions.

At Site 798, the V/Cr ratios of greater than 2.0 suggest anoxic to suboxic conditions at 1.349–1.356 and 1.389–1.396 Ma (Fig. 7), according to Jones and Manning (1994).

In the intervals of 1.349–1.356 and 1.389–1.396 Ma, the benthic faunas indicated oxic conditions. At 1.356 Ma (135.95 meters below the seafloor [mbsf]; 128-798B-15H--3W, 39–41 cm), the foraminifer assemblage was dominated by *Brizalina pacifica* [= *Bolivina pacifica* of Kato (1992); Usami et al., 2013], which accounted for 34% of all the foraminifera (Kato, 1992). *Epistominella pulchella*, which was the subordinate species, composed 33% of the assemblage. Because the relative abundance of the dominant species was not markedly higher than that of the subordinate species, we describe this as an assemblage with an indistinct dominant

https://doi.org/10.1017/qua.2017.68 Published online by Cambridge University Press

Table 2. Duration of the Temperate Intermediate Water (TIW) during the early Pleistocene and late Pliocene. The bottom and top of the TIW taxa were the geologic ages of the midpoint between samples with and without the taxa. Irizuki et al. (2007) estimated the age of samples using two types of the age model. In the Kuwae data, the time ranges are shown in the bottom, top, and duration of factor 1, which indicates the TIW.

Locality	Bottom (age; Ma)	Top (age; Ma)	Duration (ka)	Marine Oxygen Isotope Stage (MIS)
U1426	1.344	1.352	8.0	MIS 43
U1426	1.5265	1.5335	7.0	MIS 51–MIS 52
U1426	1.5785	1.5815	3.0	MIS 54
U1426	1.6205	1.623	2.5	MIS 56
U1426	1.647	1.6505	3.5	MIS 58
U1426	1.6695	1.671	1.5	MIS 59
U1426	1.739	1.7405	1.5	MIS 61
U1426	1.7575	1.7595	2.0	MIS 63
U1426	1.7695	1.7705	1.0	MIS 63
U1426	1.906	1.913	7.0	MIS 72
U1426	1.9235	1.927	3.5	MIS 73
Kuwae Formation	2.794–2.834	2.786–2.824	7.5–10.0	G11
Kuwae Formation	2.846–2.905	2.823–2.874	23.5–31.5	G13
Kuwae Formation	2.894–2.969	2.865–2.930	29.0–39.0	G15
Kuwae Formation	2.862–2.925	2.858–2.920	4.0–5.5	G15
Kuwae Formation	2.922–3.007	2.920–3.004	2.0–3.0	G16
Kuwae Formation	2.908–2.988	2.905–2.984	3.5–4.0	G16
Kuwae Formation	2.902–2.981	2.897–2.973	5.5–8.0	G16
Kuwae Formation	2.959–3.058	2.928–3.015	31.5–42.5	G18
Kuwae Formation	2.984–3.091	2.964–3.063	20.5–27.5	G19

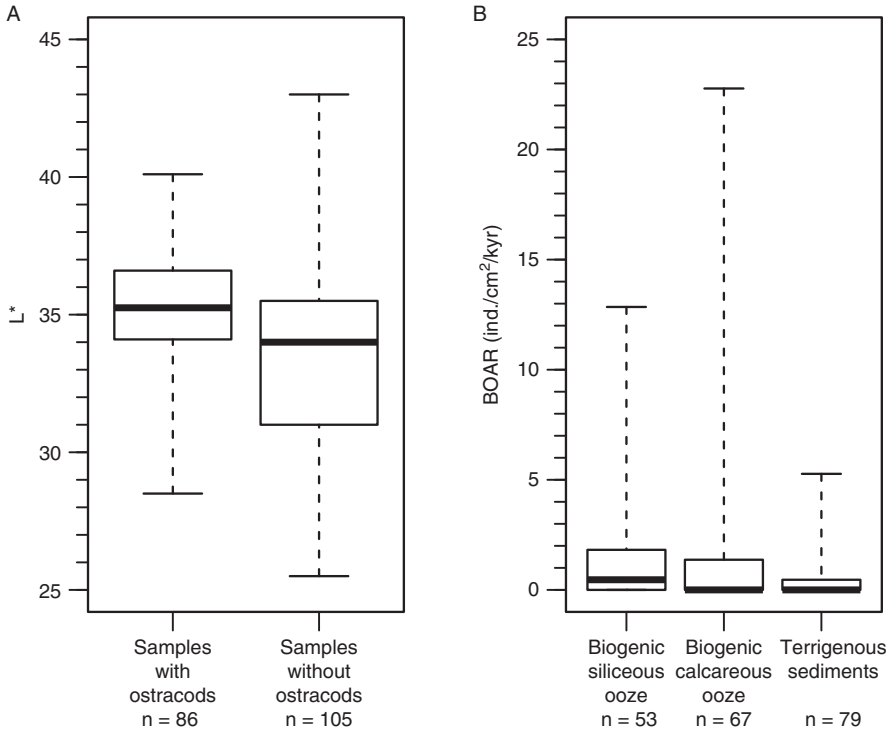

Figure 5. (A) Color reflectance parameter L* values of samples with and without ostracods. (B) Benthic Ostracoda accumulation rate (BOAR) values of biogenic siliceous and calcareous oozes and terrigenous sediment; n represents the number of samples.

https://doi.org/10.1017/qua.2017.68 Published online by Cambridge University Press

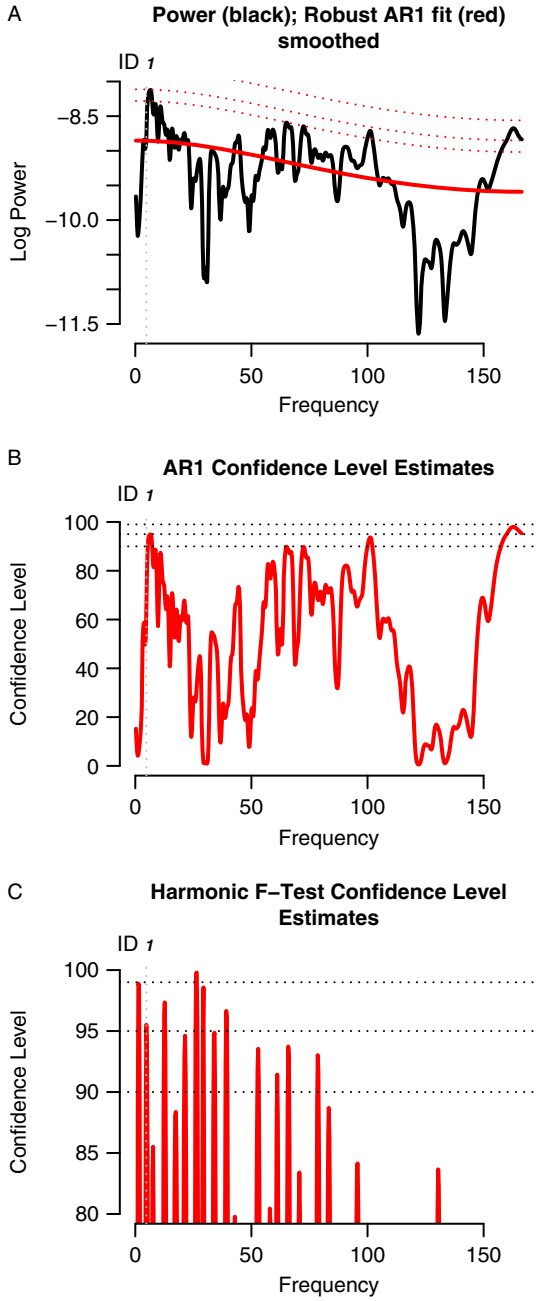

Figure 6. Multitaper method (MTM) spectra and confidence level estimates for the time series data of the Temperate Intermediate water taxa. (A) MTM power spectrum shown as a black curve. The thick red curve represents the background using the robust AR1 model. The dotted curves correspond to confidence levels of 90%, 95%, and 99% using the robust AR1 model. (B) Confidence level estimates using the robust AR1 model. (C) Confidence level estimates using the MTM harmonic *F*-test. The numerals are used to identify the significant frequencies. The significant frequencies sand their probabilities are shown in Table 4. AR1, autoregressive-1. (For interpretation of the references to color in this figure legend, the reader is referred to the web version of this article.)

species, as defined by Usami et al. (2013). The foraminifer assemblage indicated oxic conditions and relatively low productivity (Usami et al., 2013). At 1.392 Ma (140.46 m bsf; 128-798B-15H-6W, 40–42 cm), an assemblage dominated by *Angulogerina ikebei* [= *A. kokozuraensis* of Kato (1992); Usami et al., 2013] was found (Kato, 1992), which suggests oxic conditions (Usami et al., 2013). Ostracods were found at 1.326 and 1.34–1.37 Ma. Living ostracods are found at an oxygen content of greater than 0.4 mL O_2/L off Benguela in the southeastern Atlantic Ocean (Dingle, 1995). Zhou and Ikeya (2002) and Ozawa (2004) reported the absence of ostracods in the oxygen minimum zone with an oxygen content of less than 1.8 and 1.0 mL O_2/L in Suruga Bay and the Sea of Okhotsk, respectively. We consider that the occurrence of ostracods indicates an oxygen content of greater than 1.0 mL O_2/L around the Japanese Islands. The oxygen contents were estimated to be greater than 1.0 mL O_2/L. The L* values were higher than the median, which reflects the oxidizing conditions. The high V/Cr ratios are less than 2.0, indicating the oxic condition. As Piper and Isaacs (1995, 1996) considered, the high V/Cr ratios and Mo, U, and V contents were caused by sulfate-reducing and less denitrified conditions. Alternatively, as Rimmer (2004) suggested, the high contents of the chemical elements may indicate relatively low-oxygen conditions.

The occurrence of ostracods is linked to the blooming of phytoplankton. The biogenic oozes—namely, both biogenic siliceous and biogenic calcareous oozes—had significantly higher BOAR values than the terrigenous sediments, which contained fewer fossil phytoplankton (Fig. 5B; Table 3). In general, the blooming of phytoplankton leads to an increase in meiobenthic productivity (e.g., Levin et al., 2001). The results of statistical analysis indicate that the type of phytoplankton (diatoms or coccoliths) does not clearly affect BOAR values. Hyun et al. (2007) investigated the carbonate, opal, and total organic carbon (TOC) contents in the Quaternary sediments of the Sea of Japan and inferred that the blooming of diatoms provides more nutrients on the seafloor than that of coccoliths. The export productivity could vary between the blooming of diatoms and coccoliths. The BOAR values for biogenic siliceous ooze were as high as those for biogenic calcareous ooze (Fig. 5B, Table 3), which suggests that the BOAR values do not clearly depend on the type of phytoplankton. At the Oki Ridge, the changes in BOAR values at Site U1426 were not consistent with those in BFAR values at ODP Site 798 (Fig. 8). The relationship between the BOAR and food supply has been disputed (Yasuhara et al., 2012; Stepanova and Lyle, 2014). Yasuhara et al. (2012), who examined the correlation between the BOAR values and TOC content in the Quaternary sediments of the Shatsky Rise in the northern Pacific, concluded that the TOC content in the sediment displayed a hump-shaped relationship with the BOAR. On the other hand, Stepanova and Lyle (2014) recognized high BOAR values during the glacial periods with high TOC contents at an eastern equatorial Pacific site. They considered that a high food supply increased the abundance of ostracods. Our results suggest that the BOAR values exhibited a weak correlation with the export productivity, as Yasuhara et al. (2012) pointed out.

https://doi.org/10.1017/qua.2017.68 Published online by Cambridge University Press

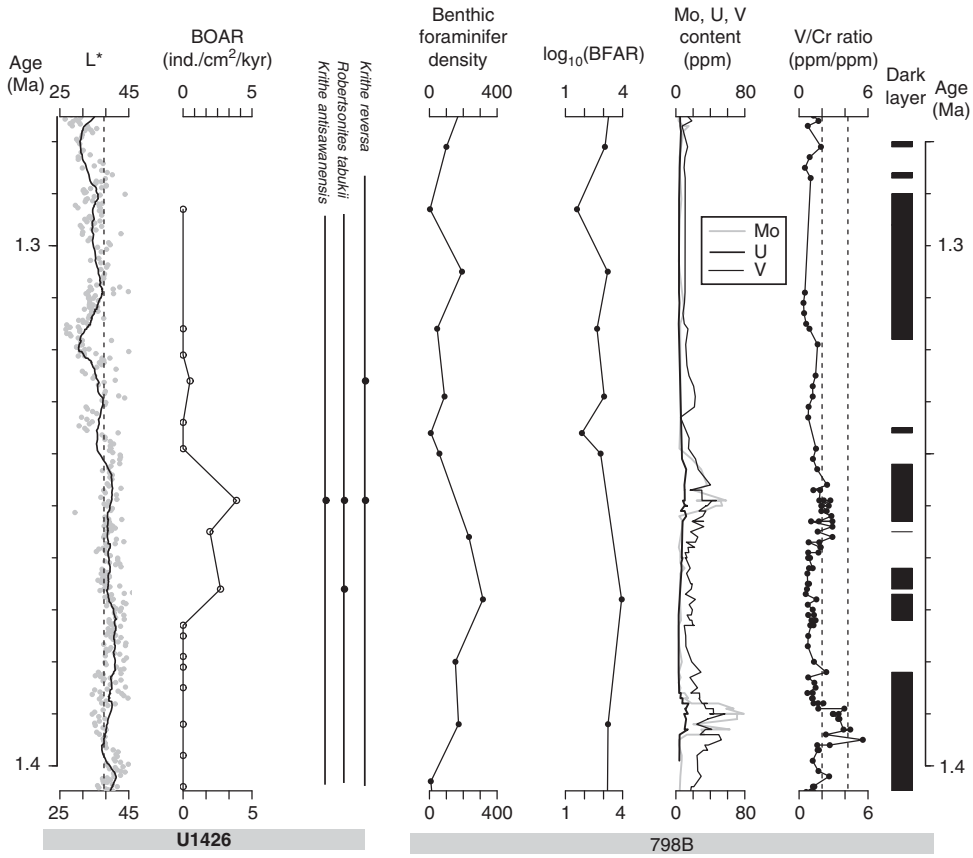

Figure 7. Plots of color reflectance parameter L*, benthic Ostracoda accumulation rate (BOAR), and dominant ostracod taxa at Site U1426 and of the benthic foraminifer accumulation rate (BFAR), species richness, geochemical elements (Mo, U, and V; ppm), V/Cr ratio (ppm/ppm), and distribution of the dark layers at Hole 798B between 1.4 and 1.2 Ma. The curve for L* represents a 10-point moving average. The dashed line indicates the median value of 34.6. The L* values were sourced from Tada et al. (2015). For the V/Cr ratio, the dashed lines indicate values of 2.0 and 4.25. The benthic foraminifer data are from Kato (1992), whereas the geochemical and dark-layer data are from Piper and Isaacs (1996).

Changes in water mass structure

In the relative abundance of the radiolarian subtropical water taxa, Motoyama et al. (2016) indicated that the subtropical water taxa account for 21–30% of radiolarian assemblages in the Holocene sediments near the Oki Ridge (samples 34, 46, 49, and 50). At Site 1426, the subtropical water taxa frequently exceed 10% above ~58 m CCSF-D patched Ver1 (Itaki, T., Sagawa, T., Kubota, Y., unpublished data). The Pleistocene subtropical water taxa indicate 0.3–9.7%. Their relative abundance suggests a smaller influx of the TWC than the modern influx. As Kitamura and Kimoto (2006) pointed out, the TWC influx has increased since the Pleistocene. Here we consider that relative abundance of more than 1% indicates the TWC flow over the Oki Ridge.

Though the middle bathyal zone, the ostracod TIW taxa often appear. The TIW taxa remained for a shorter period than those in the Pliocene Kuwae Formation (Table 2). The TIW taxa persisted for 1–8 ka at Site U1426. If *Krithe* spp. are included in the TIW taxa, these taxa persisted for 1–10 ka. The Pliocene TIW taxa remained for 2.0–42.5 ka (Irizuki et al., 2007). Even the occurrence of *G. inflata* was not consistent with that of the TIW taxa on Oki Ridge sites. The differences in duration and combination in the water mass between Site U1426 and the Kuwae Formation were caused by the bathymetric setting. The Kuwae Formation contains shallower deposits than Site U1426. The Kuwae sediments were in the lower sublittoral to upper bathyal zones shallower than ~800 m depth. The appearances of the TIW taxa indicate that the TIW possibly has developed to a greater extent than in a shallower setting.

We recognize four modes in the pattern of the radiolarian subtropical water taxa, *G. ruber*, and the ostracod faunas and infer paleoceanography (Fig. 9). Mode 1 is the intervals without the subtropical water taxa, *G. ruber*, and ostracods. The TWC did not flow over the Oki Ridge. The seafloor was exposed on the intermediate water with low oxygen content. Mode 1 fell in Marine Oxygen Isotope Stage (MIS) 40, early MIS 47–late MIS 48, late MIS 61, and MIS 63. Mode 2 is defined as the interval with the combination of ostracod JSIPW taxa and the TWC indicator, the radiolarian subtropical water taxa or *G. ruber*. The ostracod JSIPW taxa often associate with the TIW taxa. The mode occurred during late MIS 47, early MIS 49, MIS 51, MIS 54, late MIS 55, MIS 57, late MIS 58,

https://doi.org/10.1017/qua.2017.68 Published online by Cambridge University Press

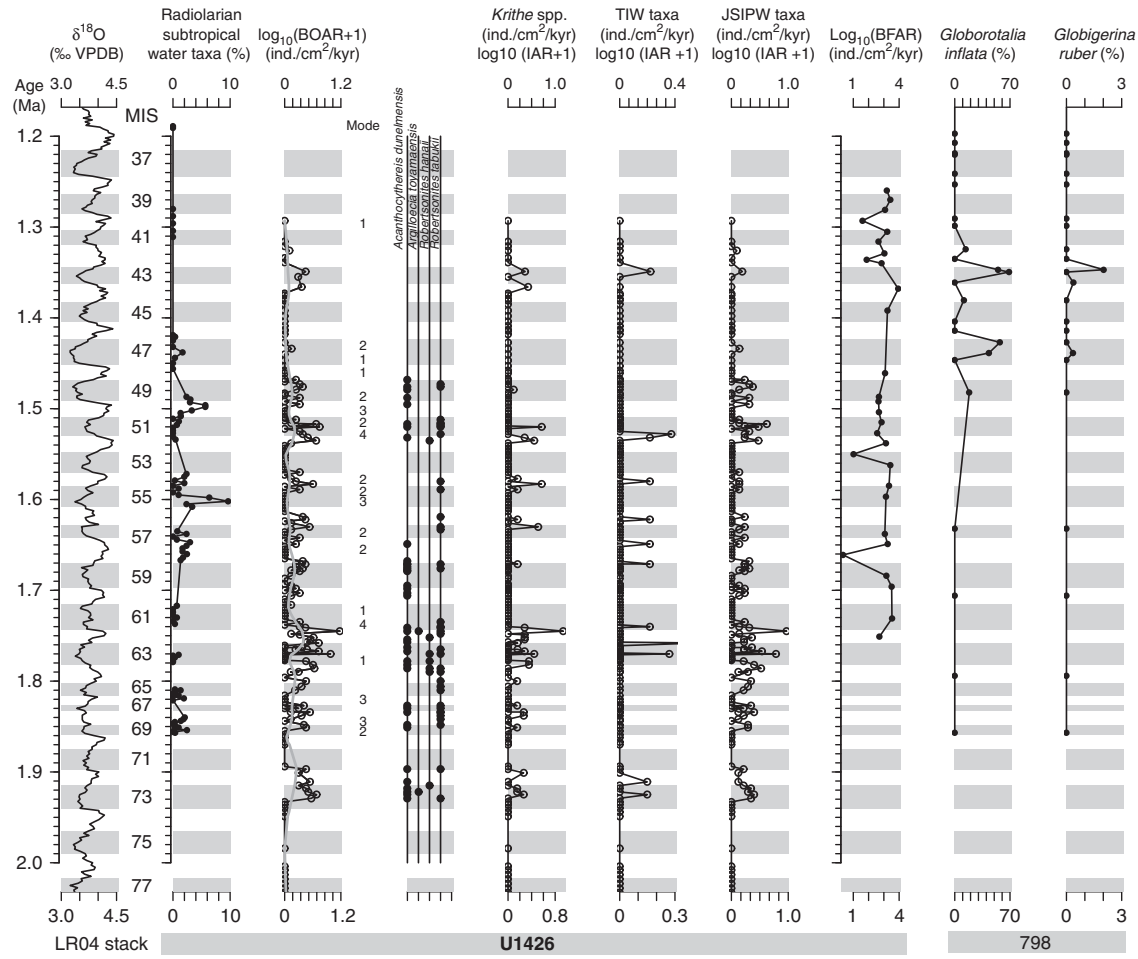

Figure 8. Plots of benthic foraminiferal $\delta^{18}O$ of the LR04 stack (Lisiecki and Raymo, 2005), the radiolarian subtropical taxa, benthic Ostracoda accumulation rate (BOAR), ostracod taxa, and accumulation rates of *Krithe* spp., the Temperate Intermediate Water (TIW) taxa, and Japan Sea Intermediate–Proper Water (JSIPW) taxa at Site U1426 and of the benthic foraminifer accumulation rate (BFAR) and relative abundances of *Globorotalia inflata* and *Globigerina ruber* at Hole 798B. IAR indicates the individual accumulation rate. The gray areas indicate interglacial stages. The BFAR and planktic foraminiferal data were sourced from Kato (1992) and Kheradyar (1992), respectively. For the BOAR data, the thick gray line indicates the LOWESS (locally weighted scatterplot smoothing)-filtered curve. VPDB, Vienna Pee Dee belemnite.

and MIS 69. In the mode, the TWC flowed over the Oki Ridge and ventilated in the north of the Sea of Japan to form the JSIPW. During MIS 54 and late MIS 58, the TIW developed and extended to the middle bathyal zone. The temperature gradient of the water column was reduced temporally. Irizuki et al. (2007) consider that the strong East Asian winter monsoon would force the temperature gradient steep and drive the TIW to be shrunken. The temporal development of the TIW was possibly caused by occasional weakening of the winter monsoon. During the intervals with the TIW taxa, temperature gradients became gentle in the water column and the TIW expanded. Mode 3 is the interval of the subtropical water taxa without ostracod faunas. It fell in MIS 50, early MIS 55, MIS 66, and MIS 68. The subtropical water taxa indicate that the TWC influx would ventilate in the north of the Sea of Japan to form intermediate water with high oxygen content. The intermediate water could not covey oxygen into deep water. The ventilation of the surface water mass was possibly shallower than mode 2. Mode 4 is the interval of the ostracod fauna without the radiolarian subtropical taxa during early MIS 51 and MIS 61. The sea surface over the Oki Ridge was not influenced by the TWC. Ostracods indicate oxic bottom water. During the early MIS 51, temperature gradients were reduced in the water column and the TIW expanded.

The power spectra indicate changes in TIW values in cycles of ~15 ka (Fig. 6, Table 4). It is not a typical periodicity of the orbital precession such as 19 and 23 ka in the East Asian monsoon (Sun et al., 2006; Ao et al., 2011) or the early Pleistocene dominant periodicity, 41 ka, which represents the orbital eccentricity. The periodicity of 41 ka is observed in changes in shallow-marine faunas (e.g., Kitamura et al. 1994; Takata, 2000; Ozawa and Kamiya, 2001). Irizuki et al. (2007) hypothesize that a weak East Asian winter monsoon would force temperature gradients to become gentler and cause the development of the TIW. The seafloor environments were affected by food supply and oxygen content that were conveyed from the sea surface. Even the Holocene dark layers have variable fabric, bioturbation, and geochemical and paleontological compositions,

https://doi.org/10.1017/qua.2017.68 Published online by Cambridge University Press

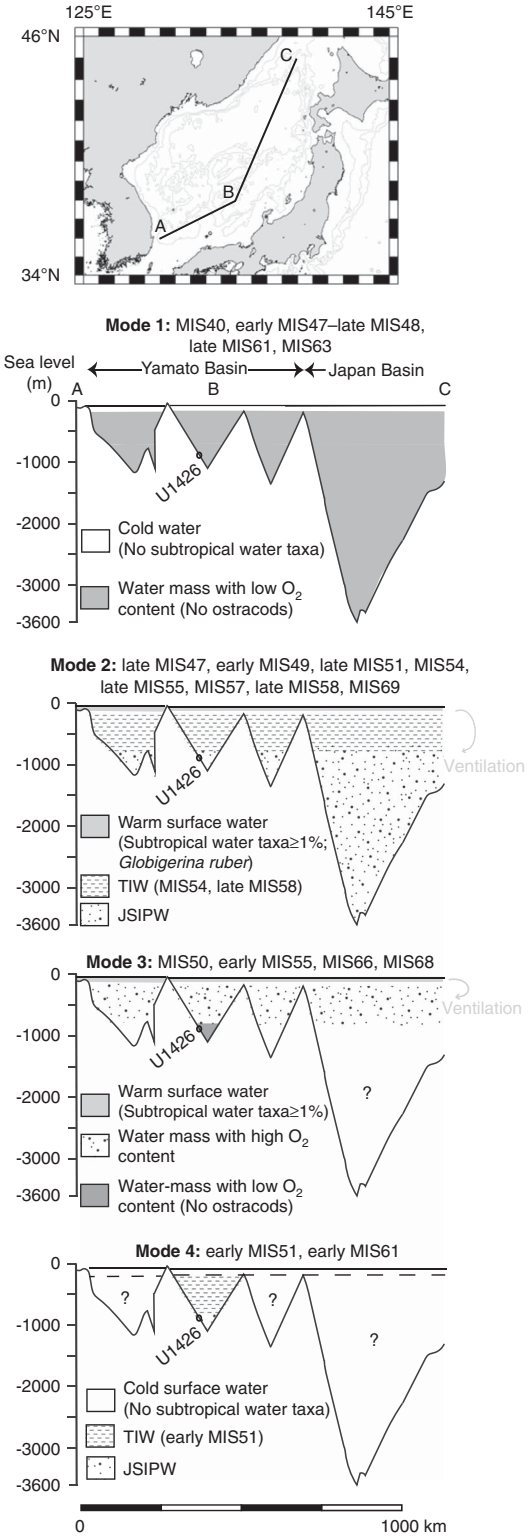

Figure 9. Schematic representation of vertical circulation in the Japan Sea. The topography is at the present. JSIPW, Japan Sea Intermediate–Proper Water; MIS, Marine Oxygen Isotope Stage; TIW, Temperate Intermediate Water.

indicating variable seafloor environments (e.g., Watanabe et al., 2007; Usami et al., 2013). The TIW periodicity resulted from the confluence of food supply and oxygen content, as well as a temperature gradient in the water column.

Table 3. Results of the Steel-Dwass test with the Monte Carlo simulation. Single and double asterisks indicate significance at levels of $P < 0.05$ and $P < 0.01$, respectively.

Comparison	*t* value	*P* value	
Biogenic siliceous ooze vs. biogenic calcareous ooze	0.841	0.159	
Biogenic siliceous ooze vs. terrigenous sediment	1	0	**
Biogenic calcareous ooze vs. terrigenous sediment	0.973	0.027	*

Deep-sea ostracod faunas through 1.7 Ma

At 1.7 Ma, the taxonomic composition did not undergo a clear change. Throughout the time interval of 1.0–2.0 Ma, the faunas consisted of the TIW and JSIPW taxa. The formation and structure of the intermediate water did not change at ~ 1.7 Ma. On average, the BOAR values exhibited a decline. The LOWESS-filtered BOAR values exhibited an obvious decrease from 1.7 to 1.6 Ma (Fig. 8). The BOAR values are linked with the food supply, as was discussed previously. The decrease in BOAR values suggests an alteration in the food supply from the sea surface. According to the model of Itaki (2016), the inflow of the TWC with a high nutrient content was enhanced after 1.7 Ma. The decrease in BOAR values may have resulted from a high nutrient content that was transported by the enhanced inflow of the TWC.

Migration of ostracods in response to changes in climate

The Japan Sea Intermediate Water conveys oxygen into the deep sea. This oxygen is easily available for deep-sea animals. In general, the deep-sea faunas are adapted to cold conditions and are scanty eurybathic species as a result of the repeated environmental changes in the Plio-Pleistocene (Kojima et al., 2007; Malyutina and Brandt, 2013). During the glacial periods, the whole of the Sea of Japan was isolated and conditions became anoxic in deep water, which might have eliminated most of the benthic faunas. Shallow-marine ostracods exhibit clear changes in taxonomic composition in response to the interglacial and glacial environmental changes (e.g., Ozawa and Kamiya, 2001; Yamada et al., 2002). Irizuki et al. (2007) hypothesized that the faunal changes could have been caused by bathymetric migration of ostracod taxa. To test this hypothesis, it is necessary to compare the taxonomic compositions of shallow-marine and deep-sea faunas.

Our data indicate the disappearance and appearance of ostracod faunas in response to deep-sea environmental changes (Fig. 4). In the interval with the radiolarian subtropical water taxa, we found *Acanthocythereis dunelmensis*, *Argilloecia*

https://doi.org/10.1017/qua.2017.68 Published online by Cambridge University Press

Table 4 . Results of applying the multitaper method to the time series data of the Temperate Intermediate Water values. ID is shown in Figure 6. AR1, autoregressive-1.

ID	Frequency (cycles/Ma)	Period (ka)	Probability (%) robust AR1	Harmonic *F*-test
1	65.87302	15.2	93.73	90.07

toyamaensis, *Robertsonites hanaii*, and *R. tabukii*, which are diagnostic for the JSIPW (Fig. 8). The occurrence of the ostracod species with the subtropical water taxa suggests that these species appeared in the deep sea during the interglacial periods. They appeared during MIS 73, MIS 67, MIS 63, MIS 53, MIS 51, and MIS 49. The four species have already been reported in the shallow-marine Omma and Hamada formations exposed on the coasts of the Sea of Japan (Cronin and Ikeya, 1987; Ozawa, 1996; Ozawa and Kamiya, 2001; Ozawa and Domitsu, 2010). These outcrops consist of coastal and shelf sediments of which the ages range from 2.0 to 1.2 Ma (e.g., Ozawa and Kamiya, 2005). The species occur in the intervals of both the interglacial and glacial periods. The occurrence of the four species at Site U1426 indicates an expansion of their habitats into deep-sea floors during the transitions from the glacial to the interglacial periods. During the glacial periods, dark-colored sediments were formed under low-oxygen conditions with low export productivity. The ostracods could not survive on the deep-sea floors. The taxa limited their habitats to shelves and coasts.

The model of migration is consistent with the hypothesis of Irizuki et al. (2007) on the migration of the taxa in response to the glacial–interglacial environmental changes. Irizuki et al. (2007) recognized decreases in the relative abundance of *A. dunelmensis* and *R. tabukii* during the interglacial periods and inferred the bathymetric migration of the taxa in response to the Pliocene changes in sea level and water mass. According to their work, the decrease in the relative abundance of *A. dunelmensis* and *R. tabukii* was attributable to migration to deeper seafloors during the developments in the TIW from the glacial to the interglacial periods. However, Irizuki et al. (2007) neither documented faunal changes in both deep-sea and shallow-marine settings nor described the species composition in the glacial deep-sea sediments. The correlation of ostracod faunas between our deep-sea data and the reported shallow-marine data enable us to corroborate the hypothesis of Irizuki et al. (2007).

Today, *A. dunelmensis, A. toyamaensis, R. hanaii,* and *R. tabukii* are not living in shelf and coastal environments in the Japan Sea (Ozawa, 2003). These species flourish in colder conditions than the TWC. The TWC inflow has increased since 1.7 Ma (Kitamura and Kimoto, 2006; Gallager et al., 2015; Itaki, 2016). It has been accompanied by increases in sea surface temperature. We consider that the increases in the temperature dismissed them from the shelf and coastal environments. Ozawa and Kamiya (2005) recognized the disappearance of 24 shallow-marine taxa in the Japan Sea after 1.5 Ma. They called the extinct taxa the "now-extinct species" and inferred that increase in amplitude of the eustatic change gave a stress to shallow-marine taxa and could have caused the extinction of the now-extinct species. *A. dunelmensis*, *A. toyamaensis*, *R. hanaii*, and *R. tabukii* are not included in the now-extinct species. The high amplification of sea level changes possibly also caused their disappearance in shallow-marine environments.

CONCLUSIONS

We revealed changes in the fauna of deep-sea ostracods that were correlated with the glacial–interglacial environmental changes.

The occurrence of the deep-sea ostracods was linked with redox conditions on the seafloors and export productivity because more ostracods were found at higher L* values and in biogenic sediments. The benthic foraminifera and redox-sensitive elements indicate that the ostracods were found in intervals with oxic conditions but were absent in intervals with dysoxic conditions.

Under a small influx of the TWC to the Sea of Japan, the JSIPW was formed. The ostracod faunas indicate expansion of the TIW to the middle bathyal zone during MIS 43, MIS 51, MIS 54, MIS 58, MIS 61, MIS 63, MIS 72, and MIS 73. The TIW suggests a gentler temperature gradient in the water column than the modern gradient. By analogy with the relationship between the modern JSIPW and the winter monsoon, the occasional expansion of the TIW was possibly caused by a weakened winter monsoon. The temporal change in the TIW taxa shows the ~ 15 ka periodicities that resulted from a confluence of temperature gradient in the water column, oxygen content, and food supply.

From 1.7 to 1.6 Ma, the taxonomic composition did not indicate changes, but the BOAR values decreased markedly, which suggests an alteration in export productivity.

The repeated appearance and disappearance of the JSIPW taxa indicates changes in their habitat ranges in response to the glacial–interglacial environmental changes. During the interglacial periods, the taxa expanded their habitats to deep-sea floors. During the glacial periods, they were eradicated from deep-sea floors, and their habitats became restricted to coastal and shelf environments.

ACKNOWLEDGMENTS

This research used samples provided by the IODP. This work involves KK's undergraduate thesis at Shinshu University. We express our thanks to Profs. Koichi Hoyanagi and Kohki Yoshida (Shinshu University, Japan) for their discussion throughout this study; Dr. Ryoichi Nakada (Japan Agency for Marine-Earth Science and Technology, Kochi) for suggestions on geochemical proxies for the redox conditions; Profs. Ryuji Tada (University of Tokyo, Japan), Takahiro Kamiya (Kanazawa University, Japan), and Dr. Tomohisa Irino (Hokkaido University, Japan) for their suggestion on stratigraphy and physical properties at the site, as well as ostracods; and Dr. Hirokazu Ozawa (Nihon University, Japan) and an anonymous reviewer for their critical reviews and constructive comments. Also, we would like to thank Enago (http://www.enago.jp) for the English-language review.

SUPPLEMENTARY MATERIAL

To view supplementary material for this article, please visit https://doi.org/10.1017/qua.2017.68

REFERENCES

Ao, H., Dekkers, M.J., Qin, L., Xiao, G., 2011. An updated astronomical timescale for the Plio-Pleistocene deposits from South China Sea and new insights into Asian monsoon evolution. *Quaternary Science Reviews* 30: 1560–1575.

Ayress, M., Barrows, T., Passlow, V., Whatley, R., 1999. Neogene to Recent species of *Krithe* (Crustacea: Ostracoda) from the Tasman Sea and off southern Australia with description of five new species. *Records of the Australian Museum* 51: 1–22.

Braeckman, U., Vanaverbeke, J., Vincx, M., van Oevelen, D., Soetaert, K., 2013. Meiofauna metabolism in suboxic sediments: currently overestimated. *PLoS One* 8: e59289. http://dx.doi.org/10.1371/journal.pone.0059289.

Chang, F., Zhouang, L., Li, T., Yan, J., Cao, Q., Cang, S., 2003. Radiolarian fauna in surface sediments of the northeastern East China Sea. *Marine Micropaleontology* 48: 173–194.

Coles, G.P., Whatley, R.C., Moguilevsky, A., 1994. The ostracod genus *Krithe* from the Tertiary and Quaternary of the North Atlantic. *Palaeontology* 37: 71–120.

Cronin, T.M., Boomer, I., Dwyer, G.S., Rodriguez-Lazaro, J., 2002. Ostracoda and paleoceanography. In: Holmes, J., Chivas, A.R. (Eds.), *The Ostracoda: Applications in Quaternary Research*. American Geophysical Union, Washington, DC, pp. 99–119.

Cronin, T.M., Ikeya, N., 1987. The Omma-Manganji ostracod fauna (Plio-Pleistocene) of Japan and the zoogeography of circumpolar species. *Journal of Micropalaeontology* 6: 65–88.

Cronin, T.M., Kitamura, A., Ikeya, N., Watanabe, M., Kamiya, T., 1994. Late Pliocene climate change 3.4-2.3 Ma: paleoceanographic record from the Yabuta Formation, Sea of Japan. *Palaeogeography, Palaeoclimatology, Palaeoecology* 108: 437–455.

Delucchi, K.L., Bostrom, A., 2004. Methods for analysis of skewed data distributions in psychiatric clinical studies: working with many zero values. *American Journal of Psychiatry* 161: 1159–1168.

Dingle, R.V., 1995. Continental shelf upwelling and benthic Ostracoda in the Benguela System (southeastern Atlantic Ocean). *Marine Geology* 122: 207–225.

Domitsu, H., Oda, M., 2005. Japan Sea planktic foraminifera in surface sediments: geographical distribution and relationships to surface water mass. *Paleontological Research* 9: 255–270.

Gallagher, S.J., Kitamura, A., Iryu, Y., Itaki, T., Koizumi, I., Hoiles, P.W., 2015. The Pliocene to recent history of the Kuroshio and Tsushima Currents: a multi-proxy approach. *Progress in Earth and Planetary Science* 2: 17. http://dx.doi.org/10.1186/s40645-015-0045-6.

Gamo, T., Momoshima, N., Tolmachyov, S., 2001. Recent upward shift of the deep convection system in the Japan Sea, as inferred from the geochemical tracers tritium, oxygen, and nutrients. *Geophysical Research Letters* 28: 4143–4146.

Hamano, Y., Krumsiek, K.A.O., Vigliotti, L., Wippern, J.J.M., 1992. Pliocene-Pleistocene magnetostratigraphy of sediment cores from the Japan Sea. In: Proceedings of the Ocean Drilling Program. Vol. 127/128, Part 2: Scientific Results. Ocean Drilling Program, College Station, TX, pp. 969–982.

Herguera, J.C., Berger, W.H., 1991. Paleoproductivity from benthic foraminifera abundance: glacial to postglacial change in the west-equatorial Pacific. *Geology* 19: 1173–1176.

Hyun, S., Bahk, J.J., Suk, B.-C., Park, B.-K., 2007. Alternative modes of Quaternary pelagic biosiliceous and carbonate sedimentation: a perspective from the East Sea (Japan Sea). *Palaeogeography, Palaeoclimatology, Palaeoecology* 247: 88–99.

Ikehara, K., 1991. Modern sedimentation of San'in district in the southern Japan Sea. In: Takano, K. (Ed.), *Oceanography of Asian Marginal Seas*. Elsevier, Amsterdam, pp. 143–162.

Ikehara, K., 2015. Marine tephra in the Japan Sea sediments as a tool for paleoceanography and paleoclimatology. *Progress in Earth and Planetary Science* 2: 36. http://dx.doi.org/10.1186/s40645-015-0068-z.

Ingle, J.C.J., Suyehiro, K., von Breymann, M.T. (Eds.), 1990). Proceedings of the Ocean Drilling Program. Vol. 128, Initial Reports. Ocean Drilling Program, College Station, TX.

Irizuki, T., Kusumoto, M., Ishida, K., Tanaka, Y., 2007. Sea-level changes and water structures between 3.5 and 2.8 Ma in the central part of the Japan Sea borderland: analyses of fossil Ostracoda from the Pliocene Kuwae Formation, central Japan. *Palaeogeography, Palaeoclimatology, Palaeoecology* 245: 421–443.

Itaki, T., 2007. Historical changes of deep-sea radiolarians in the Japan Sea during the last 640 ka. [In Japanese with English abstract.], *Fossils (Palaeontological Society of Japan)* 82: 43–51.

Itaki, T., 2016. Transitional changes in microfossil assemblages in the Japan Sea from the Late Pliocene to Early Pleistocene related to global climatic and local tectonic events. *Progress in Earth and Planetary Science* 3: 11. http://dx.doi.org/10.1186/s40645-016-0087-4.

Itaki, T., Ikehara, K., Motoyama, I., Hasegawa, S., 2004. Abrupt ventilation changes in the Japan Sea over the last 30 ky: evidence from deep-dwelling radiolarians. *Palaeogeography, Palaeoclimatology, Palaeoecology* 208: 263–278.

Itaki, T., Komatsu, N., Motoyama, I., 2007. Orbital- and millennial-scale changes of radiolarian assemblages during the last 220 ka in the Japan Sea. *Palaeogeography, Palaeoclimatology, Palaeoecology* 247: 115–130.

Jones, B., Manning, D.A.C., 1994. Comparison of geochemical indices used for the interpretation of palaeoredox conditions in ancient mudstones. *Chemical Geology* 111: 111–129.

Kanda, Y., 2013. Investigation of the freely available easy-to-use software "EZR" for medical statistics. *Bone Marrow Transplant* 48: 452–458.

Kato, M., 1992. Benthic foraminifers from the Japan Sea: Leg 128. In: Pisciotto, K.A., Ingle, J.C., Jr., von Breymann, M.T., Barron, J., (Eds.), Proceedings of the Ocean Drilling Program. Vol. 127/128, Part 1: Scientific Results. Ocean Drilling Program, College Station, TX, pp. 365–392.

Kheradyar, T., 1992. Pleistocene planktonic foraminiferal assemblages and paleotemperature fluctuations in Japan Sea, Site 798. In: Pisciotto, K.A., Ingle, J.C., Jr., von Breymann, M.T., Barron, J., (Eds.), Proceedings of the Ocean Drilling Program. Vol. 127/128, Part 1: Scientific Results. College Station, TX, pp. 457–470.

Kitamura, A., 2009. Early Pleistocene evolution of the Japan Sea Intermediate Water. *Journal of Quaternary Science* 24: 880–889.

Kitamura, A., Kimoto, K., 2006. History of the inflow of the warm Tsushima Current into the Sea of Japan between 3.5 and 0.8 Ma. *Palaeogeography, Palaeoclimatology, Palaeoecology* 236: 355–366.

Kitamura, A., Kondo, Y., Sakai, H., Horii, M., 1994. Cyclic changes in lithofacies and molluscan content in the early Pleistocene Omma Formation, central Japan related to the 41,000-year orbital obliquity. *Palaeogeography, Palaeoclimatology, Palaeoecology* 112: 345–361.

Kojima, S., Adachi, K., Kodama, Y., 2007. Formation of deep-sea fauna and changes of marine environment in the Japan Sea. [In Japanese with English abstract.], *Fossils (Palaeontological Society of Japan)* 82: 67–71.

Kumamoto, Y., Yoneda, M., Shibata, Y., Kume, H., Tanaka, A., Uehiro, T., Morita, M., Shitashima, K., 1998. Direct observation of the rapid turnover of the Japan Sea bottom water by means of AMS radiocarbon measurement. *Geophysical Research Letters* 25: 651–654.

Levin, L.A., Etter, R.J., Rex, M.A., Gooday, A.J., Smith, C.R., Pineda, J., Stuart, C.T., Hessler, R., Pawson, D., 2001. Environmental influences on regional deep-sea species diversity. *Annual Review of Ecology, Evolution, and Systematics* 32: 51–93.

Lisiecki, L.E., Raymo, M.E., 2005. A Pliocene-Pleistocene stack of 57 globally distributed benthic $\delta^{18}O$ records. *Paleoceanography* 20: PA1003. http://dx.doi.org/10.1029/2004PA001071.

Lombari, G., Boden, G., 1985. *Modern Radiolarian Global Distributions* (Special Publication No. 16A Cushman Foundation for Foraminiferal Research, Washington, DC.

Malyutina, M.V., Brandt, A., 2013. Introduction to SoJaBio (Sea of Japan Biodiversity Studies). *Deep Sea Research, Part II: Topical Studies in Oceanography* 86–87: 1–9. doi: 10.1016/j.dsr2.2012.08.011

Mann, M.E., Lees, J.M., 1996. Robust estimation of background noise and signal detection in climatic time series. *Climatic Change* 33: 409–445.

Meyers, S.R., 2012. Seeing red in cyclic stratigraphy: spectral noise estimation for astrochronology. *Paleoceanography* 27: PA3228. http://dx.doi.org/10.1029/2012PA00230.

Meyers, S.R., 2014. Astrochron: An R Package for Astrochronology (accessed September 12, 2016). https://cran.r-project.org/package=astrochron.

Moffitt, S.E., Hill, T.M., Roopnarine, P.D., Kennett, J.P., 2015. Response of seafloor ecosystems to abrupt global climate change. *Proceedings of the National Academy of Sciences of the United States of America* 112: 4684–4689.

Moodley, L., van der Zwaan, G., Herman, P., Kempers, L., van Breugel, P., 1997. Differential response of benthic meiofauna to anoxia with special reference to Foraminifera (Protista: Sarcodina). *Marine Ecology Progress Series* 158: 151–163.

Motoyama, I., Yamada, Y., Hoshiba, M., Itaki, T., 2016. Radioloarian assemblages in surface sediments of the Japan Sea. *Paleontological Research* 20: 176–206.

Ortakand, M.S., Hasegawa, S., Matsumoto, R., 2015. Biostratigraphic and palaeoecologic evaluation of the Japan Sea's Joetsu basin based on the study of foraminifera. *Paleontological Research* 19: 79–106.

Ozawa, H., 1996. Ostracode fossils from the late Pliocene to early Pleistocene Omma Formation in the Hokuriku district, central Japan. *Science Reports of the Kanazawa University* 41: 77–115.

Ozawa, H., 2003. Japan Sea ostracod assemblages in surface sediments: their distribution and relationships to water mass properties. *Paleontological Research* 7: 257–274.

Ozawa, H., 2004. Okhotsk Sea ostracods in surface sediments: depth distribution of cryophilic species relative to oceanic environment. *Marine Micropaleontology* 53: 245–260.

Ozawa, H., Domitsu, H., 2010. Early Pleistocene ostracods from the Hamada Formation in the Shimokita Peninsula, northeastern Japan: the palaeobiogeographic significance of their occurrence for the shallow-water fauna. *Paleontological Research* 14: 1–18.

Ozawa, H., Kamiya, T., 2001. Palaeoceanographic records related to glacio-eustatic flucuations in the Pleistocene Japan Sea coast based on ostracods from the Omma Formation. *Palaeogeography, Palaeoclimatology, Palaeoecology* 170: 27–48.

Ozawa, H., Kamiya, T., 2005. The effects of glacio-eustatic sea-level change on Pleistocene cold-water ostracod assemblages from the Japan Sea. *Marine Micropaleontology* 54: 167–189.

Piper, D.Z., Isaacs, C.M., 1995. Minor elements in Quaternary sediment from the Sea of Japan: a record of surface-water productivity and intermediate-water redox conditions. *Geological Society of America Bulletin* 107: 54–67.

Piper, D.Z., Isaacs, C.M., 1996. Instability of bottom-water redox conditions during accumulation of Quaternary sediment in the Japan Sea. *Paleoceanography* 11: 171–190.

R Core Team. 2015. *R: A Language and Environment for Statistical Computing*. R Foundation for Statistical Computing, Vienna, Austria.

Rimmer, S.M., 2004. Geochemical paleoredox indicators in Devonian–Mississippian black shales, central Appalachian basin (USA). *Chemical Geology* 206: 373–391.

Senjyu, T., 1999. The Japan Sea Intermediate Water; its characteristics and circulation. *Journal of Oceanography* 55: 111–122.

Stepanova, A., Lyle, M., 2014. Deep-sea Ostracoda from the Eastern Equatorial Pacific (ODP Site 1238) over the last 460 ka. *Marine Micropaleontology* 111: 100–117.

Sun, Y., Clemens, S.C., An, Z., Yu, Z., 2006. Astronomical timescale and palaeoclimatic implication of stacked 3.6-Myr monsoon records from the Chinese Loess Plateau. *Quaternary Science Reviews* 25: 33–48.

Tada, R., 1994. Paleoceanographic evolution of the Japan Sea. *Palaeogeography, Palaeoclimatology, Palaeoecology* 108: 487–508.

Tada, R., Irino, T., Ikehara, K., Karasuda, A., Sugisaki, S., Xuan, C., Sagawa, T., Itaki, T., Kubota, Y., Lu, S., Seki, A., Murray, R.W., Alvarez-Zarikian, C., and Exp. 346 Scientists. High-resolution and -precision correlation of dark and light layers in the Quaternary hemipelagic sediments of the Japan Sea recovered during IODP Expedition 346 (unpublished, under review).

Tada, R., Irino, T., Koizumi, I., 1999. Land-ocean linkages over orbital and millennial timescales recorded in Late Quaternary sediments of the Japan Sea. *Paleoceanography* 14: 236–247.

Tada, R., Murray, R.W., Alvarez Zarikian, C.A., the Expedition 346 Scientists. 2015. Proceedings of the Integrated Ocean Drilling Program. Vol. 346, Expedition Reports. Integrated Ocean Drilling Program, College Station, TX.

Takata, H., 2000. Paleoenvironmental changes during the deposition of the Omma Formation (late Pliocene to early Pleistocene) in Oyabe area, Toyama Prefecture based on the analysis of benthic and planktonic foraminiferal assemblages. [In Japanese with English abstract.], *Fossils (Palaeontological Society of Japan)* 67: 1–18.

Thomson, D.J., 1982. Spectrum estimation and harmonic analysis. *Proceedings of the IEEE* 70: 1055–1096.

Tribovillard, N., Algeo, T.J., Lyons, T., Riboulleau, A., 2006. Trace metals as paleoredox and paleoproductivity proxies: an update. *Chemical Geology* 232: 12–32.

Tyson, R.V., Pearson, T.H., 1991. Modern and ancient continental shelf anoxia: an overview. In: Tyson, R.V., Pearson, T.H. (Eds.),

Modern and Ancient Continental Shelf Anoxia. Geological Society, London, Special Publications 58: 1–24.

Usami, K., Ohi, T., Hasegawa, S., Ikehara, K., 2013. Foraminiferal records of bottom-water oxygenation and surface-water productivity in the southern Japan Sea during 160–15 ka: associations with insolation changes. *Marine Micropaleontology* 101: 10–27.

Watanabe, S., Tada, R., Ikehara, K., Fujine, K., Kido, Y., 2007. Sediment fabrics, oxygenation history, and circulation modes of Japan Sea during the Late Quaternary. *Palaeogeography, Palaeoclimatology, Palaeoecology* 247: 50–64.

Yamada, K., Irizuki, T., Tanaka, Y., 2002. Cyclic sea-level changes based on fossil ostracode faunas from the Upper Pliocene Sasaoka Formation, Akita Prefecture, northeast Japan. *Palaeogeography, Palaeoclimatology, Palaeoecology* 185: 115–132.

Yamada, K., Kuroki, K., Yamaguchi, T. Pliocene and Pleistocene deep-sea ostracodes from Integrated Ocean Drilling Program Site U1426 in the Sea of Japan (Expedition 346). In: Tada, R., Murray, R.W., Alvarez Zarikian, C.A., and the Expedition 346 Scientists (Eds.), Asian Monsoon. Proceedings of the Integrated Ocean Drilling Program. Vol. 346. Integrated Ocean Drilling Program, College Station, TX. (in press).

Yamada, K., Tanaka, Y., Irizuki, T., 2005. Paleoceanographic shifts and global events recorded in late Pliocene shallow marine deposits (2.80–2.55 Ma) of the Sea of Japan. *Palaeogeography, Palaeoclimatology, Palaeoecology* 220: 255–271.

Yasuhara, M., Hunt, G., Cronin, T., Hokanishi, N., Kawahata, H., Tsujimoto, A., Ishitake, M., 2012. Climatic forcing of Quaternary deep-sea benthic communities in the North Pacific Ocean. *Paleobiology* 38: 162–179.

Zhao, Q., Whatley, R., 1997. Distribution of the ostracod genera *Krithe* and *Parakrithe* in bottom sediments of the East China and Yellow Seas. *Marine Micropaleontology* 32: 195–207.

Zhou, B., Ikeya, N., 2002. The limit of low oxygen level that marine ostracods can cope with: a case study of the Suruga Bay, central Japan. *National Science Museum Monographs* 22: 89–95.

https://doi.org/10.1017/qua.2017.68 Published online by Cambridge University Press